

Heptacoordinated Nickel(II) as an Ising-Type Anisotropic Building Unit: Illustration with a Pentanuclear $[(\text{NiL})_3\{\text{W}(\text{CN})_8\}_2]$ ComplexNayanmoni Gogoi,[†] Mehrez Thljjeni, Carine Duhayon, and Jean-Pascal Sutter*

LCC (Laboratoire de Chimie de Coordination), CNRS, 205 route de Narbonne, F-31077 Toulouse, France

Université de Toulouse, UPS, INPT, LCC, F-31077 Toulouse, France

Supporting Information

ABSTRACT: Heptacoordinated nickel(II) complexes characterized by substantial Ising-type single-ion anisotropy have been involved in the construction of two pentanuclear $[\text{Ni}_3\text{W}_2]$ compounds by association with $[\text{W}(\text{CN})_8]^{3-}$. For one of them, slow relaxation of magnetization was observed to occur concomitantly with antiferromagnetic ordering.

The paradigm of molecular (nano)magnets, known as single-molecule magnets (SMMs) and single-chain magnets, has attracted tremendous interest in recent years because of its putative relevance to high-density data storage materials. This topic has also stimulated more fundamental questions with relation to the properties and chemical constructions of such materials. One topical challenge for chemists concerns control of the magnetic anisotropy by design. Access to large anisotropy appears to be essential to expect significant progress in the performances of the materials.¹ Recent reports suggest that moving from octahedral to less common geometries such as trigonal or pentagonal bipyramids can substantially increase the anisotropy for Co^{II} or Fe^{II} metal ions.^{2–7} In an extension of our investigations on heptacoordinated complexes,^{2,8} we have considered Ni^{II} and found that in D_{5h} geometry this ion exhibits substantial Ising-type anisotropy. Herein we report a series of preliminary results on such complexes and on pentanuclear heterometallic compounds involving heptacoordinated nickel units in association with $[\text{W}(\text{CN})_8]^{3-}$.

The heptacoordinated nickel complexes considered in this study are depicted in Figure 1. These are readily obtained by the reaction of a 2,6-diacetylpyridinebis(carboxylic acid hydrazone)

derivative ($\text{L}^{\text{N}_3\text{O}_2\text{R}}$) with a $\text{Ni}(\text{NO}_3)_2$ salt (see the Supporting Information, SI). The pentadentate ligand ($\text{R} = \text{Ph}$ for **1** and $\text{R} = \text{BiPh}$ for **2**) occupies five equatorial coordination sites of the Ni^{II} ion. The coordination sphere is completed by two H_2O molecules for **1** or one MeOH molecule and one NO_3^- anion for **2**, located in axial positions. A view of the crystal structure for **2**¹⁰ is given in Figure 1. The N and O atoms in equatorial positions are well located within a plane, and the distances to Ni atom range from 2.070 to 2.414 Å, thus confirming bonding of the ligand by all five atoms. The polyhedral shape around the Ni centers was ascertained by a continuous-shape measures analysis¹¹ carried out with *SHAPE*.¹² For **1** and **2**, the coordination sphere of the Ni atom adopts slightly distorted pentagonal-bipyramidal (D_{5h}) geometry (Table S2 in the SI).

The presence of labile ligands in axial positions makes **1** and **2** attractive building blocks for the construction of low-dimensional heteronuclear compounds. Their reaction with $[\text{W}(\text{CN})_8]^{3-}$, chosen because of its strong ferromagnetic interaction with Ni^{II} ,¹³ afforded the pentanuclear compounds $[\{\text{NiL}^{\text{N}_3\text{O}_2\text{Ph}}\}_3\{\text{W}(\text{CN})_8\}_2(\text{H}_2\text{O})_2] \cdot 2\text{MeCN} \cdot 12\text{H}_2\text{O}$ (**3**) and $[\{\text{NiL}^{\text{N}_3\text{O}_2\text{BiPh}}\}_3\{\text{W}(\text{CN})_8\}_2(\text{H}_2\text{O})_2] \cdot 2\text{MeCN} \cdot 9\text{H}_2\text{O}$ (**4**). The molecular structure of **3**¹⁰ (Figure 2) consists of a cyano-bridged pentanuclear cluster made up of two $[\text{W}(\text{CN})_8]$ units and three $[\text{NiL}^{\text{N}_3\text{O}_2\text{Ph}}]$ moieties in an almost linear arrangement. All of the Ni ions exhibit heptacoordinated surroundings with the pentadentate $\text{L}^{\text{N}_3\text{O}_2\text{Ph}}$ ligand in an equatorial position. The coordination sphere for the terminal Ni1 units is completed by a H_2O ligand positioned trans to the cyano ligand. The mean planes defined by one Ni atom and the coordinated atoms of $\text{L}^{\text{N}_3\text{O}_2\text{Ph}}$ are almost parallel to each other with a deviation of $1.9(1)^\circ$ for that of Ni1 and Ni2 and $3.8(1)^\circ$ between the planes containing Ni1 (Figure S4 in the SI). This neutral pentanuclear compound crystallizes with 2 MeCN and 12 H_2O molecules located in the crystal lattice. Some of these H_2O molecules establish hydrogen bonds with N atoms of the cyano ligands and act as bridges between the $[\text{Ni}_3\text{W}_2]$ molecules, leading to 2D networks (Figure S5 in the SI). We will see below that this has an effect on the magnetic behavior found for **3**. Compound **4** crystallizes in space group $P2_1$,¹⁰ and the arrangement of the pentanuclear cluster (Figure 2) is reminiscent of that of **3**. However, the five constituting units form a bent molecule. As a result, the angles between the $\{\text{NiL}^{\text{N}_3\text{O}_2\text{BiPh}}\}$ mean planes are $45.1(2)^\circ$, $40.6(1)^\circ$, and $3.5(2)^\circ$ for $\{\text{Ni1}^\wedge\text{Ni2}\}$, $\{\text{Ni1}^\wedge\text{Ni3}\}$, and $\{\text{Ni2}^\wedge\text{Ni3}\}$, respectively (Figure S6 in the SI). A quite important

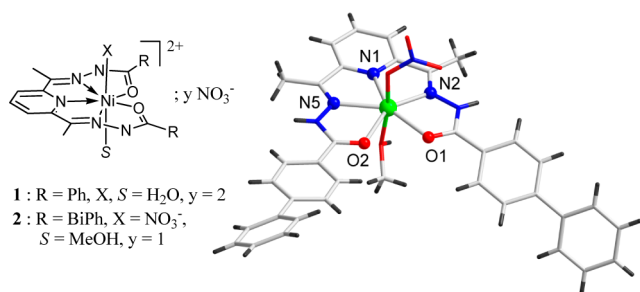


Figure 1. (left) Sketch of the ligand system for **1** and **2**. (right) Crystal structure for the cationic unit $[\text{NiL}^{\text{N}_3\text{O}_2\text{BiPh}}(\text{MeOH})(\text{NO}_3)]^+$ of **2**. For geometrical data see Figure S1 in the SI.

Received: December 12, 2012

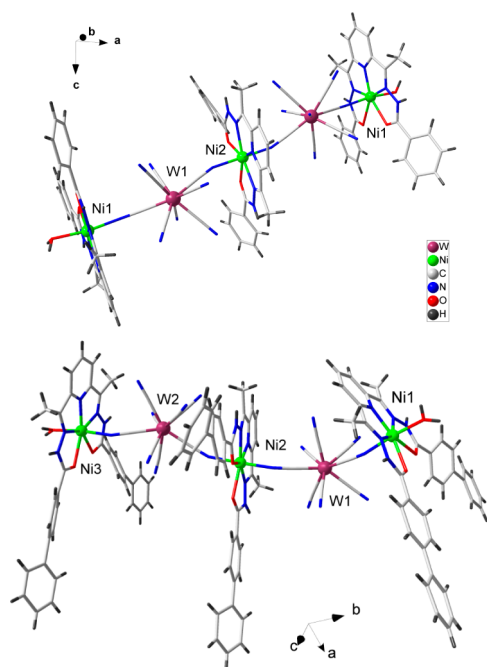


Figure 2. Crystal structures for (top) **3** and (bottom) **4** (lattice solvent molecules are not shown). Geometrical data can be found in the SI.

volume of the crystal (30%) is occupied by solvent molecules, only some of which could be identified from X-ray data. Therefore, the final refinement for the structure was done without these molecules. Interestingly, because of the steric demand of the biphenyl units, the positioning of the pentanuclear clusters in the lattice allows one to exclude the possibility of H₂O acting as a bridge between them (Figure S7 in the SI). For both **3** and **4**, the coordination spheres of the Ni centers have slightly distorted pentagonal-bipyramidal shape, while W centers are in distorted square-antiprism surroundings (Table S2 in the SI).^{11,14}

The magnetic behaviors for all compounds have been recorded on crystalline samples mixed with grease and held in a gelatin capsule. The field dependence of magnetization recorded between 2 and 10 K for **2** revealed a behavior characteristic of substantial magnetic anisotropy. As shown in Figure 3, the $M = f(H/T)$ curves do not superpose. These behaviors have been modeled with the help of MAGPACK; best fits have been obtained with $D = -12.5 \text{ cm}^{-1}$, $E = 1.2 \text{ cm}^{-1}$, and $g_{\text{iso}} = 2.22$. These values well compare to that of **1** ($D = -13.9 \text{ cm}^{-1}$, $E/D = 0.11$, and $g_{\text{iso}} = 2.26$) deduced from combined magnetization,

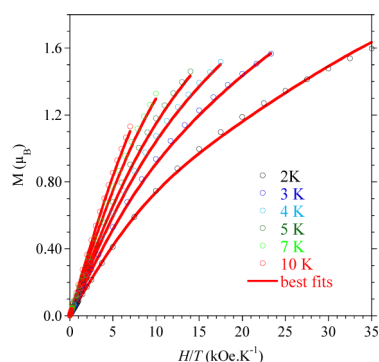


Figure 3. Field dependence of magnetization for **2**.

high-frequency electron paramagnetic resonance, and theoretical studies.¹⁵ Note that the easy axis of magnetization for these complexes is along the apical positions.¹⁵ The temperature dependence of $\chi_M T$ for **3** (Figure 4) confirms that ferromagnetic

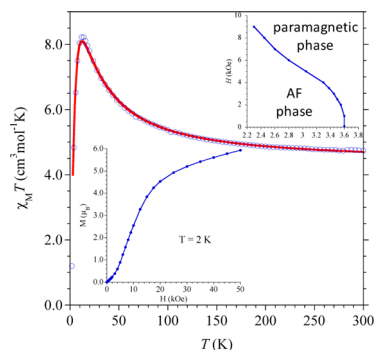


Figure 4. $\chi_M T$ versus T behavior (blue \circ) for **3** recorded with $H_{\text{dc}} = 1 \text{ kOe}$ and the best fit (red —). Inset: M versus H at 2 K and H – T phase diagram deduced from $\chi_M = f(T, H)$ data (Figure S9 in the SI).

interactions take place between the Ni and W centers. At 300 K, the value for $\chi_M T$ is $4.73 \text{ cm}^3 \text{ mol}^{-1} \text{ K}^{-1}$, slightly above the value of 4.42 anticipated for three $S = 1$ ($g = 2.22$) and two $S = 1/2$ ($g = 2.0$) centers without exchange interactions. This value continuously increases as T is lowered to reach a maximum of 8.23 at 13 K . Below this temperature, $\chi_M T$ abruptly falls to reach $2.20 \text{ cm}^3 \text{ mol}^{-1} \text{ K}^{-1}$ at 2 K . The χ_M versus T behavior also exhibits a maximum (Figure S9 in the SI), suggesting antiferromagnetic ordering. The H – T phase diagram establishes T_N at 3.6 K (Figure 4). The propagation of the intermolecular interactions is attributed to the hydrogen-bonding network formed with H₂O molecules.¹⁶ The field dependence of magnetization recorded at 2 K shows an S-shaped behavior characteristic for metamagnetism. Saturation is not reached up to 50 kOe ; this could be attributed to magnetic anisotropy. The $\chi_M T$ behavior for **4** (Figure S10 in the SI) is similar except that the value reached at 2 K is larger ($5.8 \text{ cm}^3 \text{ mol}^{-1} \text{ K}^{-1}$), and no maximum is seen for χ_M versus T . Obviously, for **4** intermolecular interactions are avoided. The magnetic susceptibilities have been computed by exact calculations of the energy levels associated with the spin Hamiltonian $[H = -J(S_{\text{Ni1}}S_{\text{W1}} + S_{\text{Ni2}}S_{\text{W1}} + S_{\text{Ni2}}S_{\text{W2}} + S_{\text{Ni3}}S_{\text{W2}}) + DS_z^2 + \sum_i g\beta HS_i]$ through diagonalization of the full matrix with a general program for axial and rhombic symmetries.¹⁷ The Ni–W exchange J_{NiW} , a mean D parameter, and intermolecular interactions in the mean-field approximation, zJ' , have been taken into account. The best fit to the experimental behavior above 4 K for **3** yielded $J_{\text{NiW}} = 32 \text{ cm}^{-1}$, $D = -15 \text{ cm}^{-1}$, $zJ' = -0.17 \text{ cm}^{-1}$, and $g = 2.16$ and that above 6 K for **4** yielded $J_{\text{NiW}} = 17.2 \text{ cm}^{-1}$, $D = -5.0 \text{ cm}^{-1}$, $zJ' = -0.34 \text{ cm}^{-1}$, and $g = 2.17$. The use of independent J_{NiW} parameters for terminal and central Ni centers did not improve the fits. Moreover, while D and zJ' are strongly correlated, both parameters were required to properly reproduce the low-temperature behavior (Figures S9 and S10 in the SI). The strengths of the Ni–W interaction for **3** and **4** compare well to the reported values.^{13,18} This is in agreement with localization of the two unpaired electrons in the s -type orbitals (d_{z^2} and $d_{x^2-y^2}$) of Ni as anticipated from the orbital energy diagram for D_{5h} symmetry. Moreover, the fittings suggest a notably larger D for **3** compared to that of **4**. The alternating-current (ac) susceptibility behaviors for **3** and **4** have been measured in the zero static field. For **3**, slow relaxation of magnetization is observed below 4 K (Figure S5), as indicated by

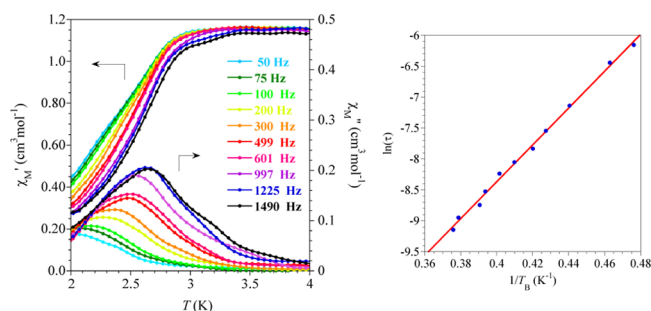


Figure 5. (left) Temperature dependence of χ_M' and χ_M'' as a function of the frequency for **3**. (right) Plot of $\ln \tau$ versus $1/T_B$. The straight line is a fit to the data points (see the text).

the frequency dependence of in-phase (χ_M') and out-of-phase (χ_M'') ac signals. It can be noticed that the χ_M'' signals are found below T_N . Such behavior was not found for **4** even when a static field was applied. In Figure 5, we plot the blocking temperatures (defined as the peak of χ_M'' for a given frequency) as $\ln \tau$ versus $1/T_B$, where $\tau = 1/2\pi\nu$ is the corresponding relaxation time for a given frequency ν . The values obtained from the least-squares fitting of the Arrhenius law ($\tau = \tau_0 \exp(\Delta/k_B T)$) are $\Delta/k_B = 30$ K and $\tau_0 = 1.6 \times 10^{-9}$ s, confirming a SMM-type behavior for **3**.

The results reported here substantiate the possibility of designing large single-ion anisotropy of a metal center by controlling the coordination geometry. Ni^{II} is known to usually exhibit positive D values in penta- or hexacoordinated geometries. In a pentagonal-bipyramidal environment imposed by the preorganized pentadentate ligand, Ni^{II} exhibits substantially negative D values. While related values are known for strongly distorted octahedral surroundings, such geometries are often difficult to design on purpose.^{19,20} A further prominent characteristic of the reported complexes is the opportunity to involve them as Ising-type building units for the design of molecular magnets. This is illustrated by **3**, for which slow relaxation of magnetization is observed concomitantly with antiferromagnetic ordering. While for **4** the intermolecular interactions have been avoided, no SMM behavior is observed. We believe that the different arrangement for this pentanuclear system is the cause. Work is in progress to expand the family of heteronuclear compounds involving heptacoordinated nickel units.

■ ASSOCIATED CONTENT

■ Supporting Information

X-ray crystallographic data in CIF format, syntheses, crystal, ORTEP, and geometrical data for **2–4**, magnetic data for **4**. This material is available free of charge via the Internet at <http://pubs.acs.org>. The atomic coordinates for **2–4** have also been deposited with the Cambridge Crystallographic Data Centre. The coordinates can be obtained, upon request, from the Director, Cambridge Crystallographic Data Centre, 12 Union Road, Cambridge CB2 1EZ, U.K., by references CCDC 892918, 892919, and 892920.

■ AUTHOR INFORMATION

Corresponding Author

*E-mail: sutter@lcc-toulouse.fr.

Present Address

[†]Department of Chemical Sciences, Tezpur University, Napaam, Sonitpur, Assam 784 028, India.

Notes

The authors declare no competing financial interest.

■ ACKNOWLEDGMENTS

This work was supported by the French Research Agency (Agence Nationale de la Recherche; Grant ANR-09-BLAN-0054-01).

■ REFERENCES

- (1) Waldmann, O. *Inorg. Chem.* **2007**, *46*, 10035–10037.
- (2) Venkatakrishnan, T. S.; Sahoo, S.; Bréfuel, N.; Duhayon, C.; Paulsen, C.; Barra, A.-L.; Ramasesha, S.; Sutter, J.-P. *J. Am. Chem. Soc.* **2010**, *132*, 6047–6056.
- (3) Batchelor, L. J.; Sangalli, M.; Guillot, R. g.; Guihéry, N.; Maurice, R.; Tuna, F.; Mallah, T. *Inorg. Chem.* **2011**, *50*, 12045.
- (4) Freedman, D. E.; Harman, W. H.; Harris, T. D.; Long, G. J.; Chang, C. J.; Long, J. R. *J. Am. Chem. Soc.* **2010**, *132*, 1224–1225.
- (5) Harman, W. H.; Harris, T. D.; Freedman, D. E.; Fong, H.; Chang, A.; Rinehart, J. D.; Ozarowski, A.; Sougrati, M. T.; Grandjean, F.; Long, G. J.; Long, J. R.; Chang, C. J. *J. Am. Chem. Soc.* **2010**, *132*, 18115.
- (6) Jurca, T.; Farghal, A.; Lin, P.-H.; Korobkov, I.; Murugesu, M.; Richeson, D. S. *J. Am. Chem. Soc.* **2011**, *133*, 15814.
- (7) Zhang, Y.-Z.; Wang, B.-W.; Sato, O.; Gao, S. *Chem. Commun.* **2010**, *46*, 6959–6961.
- (8) Pradhan, R.; Desplanches, C.; Guionneau, P.; Sutter, J.-P. *Inorg. Chem.* **2003**, *42*, 6607–6609.
- (9) Giordano, T. J.; Palenik, G. J.; Palenik, R. C.; Sullivan, D. A. *Inorg. Chem.* **1979**, *18*, 2445–2450.
- (10) Crystallographic data for **2**: $\text{C}_{36.50}\text{H}_{35}\text{N}_7\text{NiO}_{9.50}$, monoclinic, $P2_1/c$, $a = 8.3993(2)$ Å, $b = 18.0571(3)$ Å, $c = 23.6812(3)$ Å, $\alpha = 90^\circ$, $\beta = 97.872(2)^\circ$, $\gamma = 90^\circ$, $V = 3557.8(1)$ Å³, $R1 = 0.0717$ [$I > 3\sigma(I)$]. Crystallographic data for **3**: $\text{C}_{86.33}\text{H}_{93}\text{N}_{31.67}\text{Ni}_3\text{O}_{20}\text{W}_2$, monoclinic, $C2/c$, $a = 29.1095(2)$ Å, $b = 16.8728(1)$ Å, $c = 21.4170(1)$ Å, $\alpha = 90^\circ$, $\beta = 90.182(1)^\circ$, $\gamma = 90^\circ$, $V = 10519.1(1)$ Å³, $R1 = 0.0319$ [$I > 3\sigma(I)$]. Crystallographic data for **4**: $\text{C}_{121}\text{H}_{91}\text{N}_{31}\text{Ni}_3\text{O}_8\text{W}_2$, monoclinic, $P2_1$, $a = 11.0517(4)$ Å, $b = 30.978(1)$ Å, $c = 21.1989(7)$ Å, $\alpha = 90^\circ$, $\beta = 98.685(2)^\circ$, $\gamma = 90^\circ$, $V = 7174.4(4)$ Å³, $R1 = 0.0532$ [$I > 3\sigma(I)$].
- (11) Casanova, D.; Alemany, P.; Bofill, J. M.; Alvarez, S. *Chem.—Eur. J.* **2003**, *9*, 1281–1295.
- (12) Llunell, M.; Casanova, D.; Cirera, J.; Bofill, J. M.; Alemany, P.; Alvarez, S.; Pinsky, M.; Avnir, D. *SHAPE: Continuous shape measures of polygonal and polyhedral molecular fragments*; University of Barcelona: Barcelona, 2005.
- (13) Visinescu, D.; Desplanches, C.; Imaz, I.; Bahers, V.; Pradhan, R.; Villamena, F.; Guionneau, P.; Sutter, J.-P. *J. Am. Chem. Soc.* **2006**, *128*, 10202–10212.
- (14) Casanova, D.; Llunell, M.; Alemany, P.; Alvarez, S. *Chem.—Eur. J.* **2005**, *11*, 1479–1494.
- (15) Ruamps, R.; Batchelor, L. J.; Maurice, R.; Gogoi, N.; Jiménez-Lozano, P.; Guihéry, N.; de Graaf, C.; Barra, A.-L.; Sutter, J.-P.; Mallah, T. *Chem.—Eur. J.* **2013**, *19*, 950–956.
- (16) Sutter, J.-P.; Dhers, S.; Costes, J. P.; Duhayon, C. *C. R. Chim.* **2008**, *11*, 1200–1206.
- (17) Boudalis, A. K.; Clemente-Juan, J. M.; Dahan, F.; Tuchagues, J. P. *Inorg. Chem.* **2004**, *43*, 1574–1586.
- (18) Dhers, S.; Sahoo, S.; Costes, J.-P.; Duhayon, C.; Ramasesha, S.; Sutter, J.-P. *CrystEngComm* **2009**, *11*, 2078–2083.
- (19) Rogez, G.; Rebilly, J.-N.; Barra, A.-L.; Sorace, L.; Blondin, G.; Kirchner, N.; Duran, M.; van Slageren, J.; Parsons, S.; Ricard, L.; Marvilliers, A.; Mallah, T. *Angew. Chem., Int. Ed.* **2005**, *44*, 1876–1879.
- (20) Boca, R. *Coord. Chem. Rev.* **2004**, *248*, 757–815.